NATIONAL ADVISORY COMMITTEE FOR AERONAUTICS

WARTIME REPORT

ORIGINALLY ISSUED

March 1945 as Memorandum Report A5C10

INVESTIGATION OF SLIPSTREAM EFFECTS ON A WING-INLET
OIL-COOLER DUCTING SYSTEM OF A TWIN-ENGINE AIRPLANE
IN THE AMES 40- BY 80-FOOT WIND TUNNEL

By Dean R. Chapman

Ames Aeronautical Laboratory Moffett Field, California



WASHINGTON

NACA WARTIME REPORTS are reprints of papers originally issued to provide rapid distribution of advance research results to an authorized group requiring them for the war effort. They were previously held under a security status but are now unclassified. Some of these reports were not technically edited. All have been reproduced without change in order to expedite general distribution.



NATIONAL ADVISORY COMMITTEE FOR AERONAUTICS

MEMORANDUM REPORT

for the

Bureau of Aeronautics, Navy Department
INVESTIGATION OF SLIPSTREAM EFFECTS ON A WING-INLET
OIL-COOLER DUCTING SYSTEM OF A TWIN-ENGINE AIRPLANE
IN THE AMES 40- by 30-FOOT WIND TUNNEL

By Dean R. Chapman

SUMMARY

An investigation of the wing-inlet oil-cooler ducts on a twinengine airplane was conducted to determine both internal- and
external-flow characteristics of the ducting installation. Tests
were made with power on as well as with propellers removed. In
addition, ground tests of the duct passages and model tests of
various 1/2-scale revised inlets were also conducted in order to
develop a ducting system with low over-all losses throughout the
operating range.

The full-scale investigation showed that a premature separation of internal flow occurred in both left- and right-wing inlets when tested with propellers removed, but occurred only in the right-wing inlet when tested with propellers operating. In the model tests, a revised inlet design for the right wing was developed which produced satisfactory pressure recovery throughout the operating conditions. The ground tests of the ducting system showed that the losses in the diffuser were quite low even with considerable production irregularities in the fabricated parts. The increment of external drag caused by the wing inlets was found to be zero in the high-speed attitude and 0.000l in the climb attitude.

INTRODUCTION

Various aerodynamic and cooling tests have been conducted on a twin-engine airplane in the Ames 40- by 80-foot wind tunnel. An investigation of the aerodynamic characteristics of the ducting system was carried out as a part of this testing program, and the results are presented in this report.

The ducting system consists of two similar pairs of wing inlets: one to take in charge air, and another to take in air for the oil cooler. Although the results of flight tests did not indicate any trouble which could be attributed to the charge—air ducts, they did demonstrate unsatisfactory oil—cooling characteristics during a climb. The wind—tunnel investigation, therefore, was made with particular attention to the oil—cooler ducts.

The investigation was composed of four relatively independent phases involving both model and ground tests, as well as the full-scale wind-tunnel tests. These four phases were (1) full-scale tests with propellers removed, (2) full-scale tests with power on, (3) tests of 1/2-scale models of various modified wing inlets, and (4) ground tests of the duct passages. Accordingly, this report comprises those four divisions, along with a discussion of their correlation and application to other ducting systems.

COEFFICIENTS AND NOTATION

The coefficients obtained in the full-scale airplane investigation were corrected for jet-boundary interference and for the tare and interference of support struts. The data obtained in the 1/2-scale model tests were corrected for the effect of wall interference by the methods of reference 1.

The symbols used throughout the report are defined as follows:

- αu uncorrected angle of attack, referred to fuselage reference line, degrees
- p static pressure, pounds per square foot
- ρ mass density of air, slugs per cubic foot
- velocity, feet per second
- q dynamic pressure, pounds per square foot $(\frac{1}{2}\rho V^2)$
- H total head, pounds per square foot $[p + q(1 + \eta)]$
- AH loss in total head, pounds per square foot
- A cross-sectional area of duct, square feet
- n propeller speed, rps
- D diameter of propeller, feet
- S wing area, square feet

CL airplane lift coefficient (L/qS)

cl section lift coefficient at a station through center of inlet

CD; internal drag coefficient of duct

P pressure coefficient $\left(\frac{p-p_0}{q_0}\right)$

 $1 - \frac{\Delta H}{Q_Q}$ pressure-recovery coefficient

Q volume quantity of flow, cubic feet per second

Q/Vo flow coefficient, square feet

 V_1/V_0 inlet velocity ratio $\left(\frac{C}{A_1V_0} = 1.62 \frac{Q}{V_0}\right)$

 T_c thrust coefficient $\left[\begin{array}{c} effective \ thrust \ of \ both \ propellers \\ 2 \ \rho V^2 \ D^2 \end{array}\right]$

$$= \frac{S}{4D^{2}} \left(c_{D_{power off}} - c_{D_{power on}} \right)$$

$$1 + \eta$$
 compressibility factor $\left(1 + \frac{1}{4}M^2 + \frac{1}{40}M^4 + \dots\right)$

subscripts

- o free-stream conditions
- 1 conditions at station 1
- 2 conditions at station 2
- i conditions at the inlet (except in CD;)

AIRPLANE, INSTRUMENTATION AND TEST APPARATUS

The test airplane was a twin-engine, single-place, midwing fighter designed for both land- and carrier-based operations. It is powered by two R-2800-22 engines, having a military rating of 2100 horsepower at 2800 rpm. Each of the engines operated a three-blade propeller 13 feet 2 inches in diameter. A three-view drawing showing the principal dimensions of the airplane is presented as figure 1.

Figure 2, a schematic drawing of the duct passages, shows the various station designations which were used throughout the investigation. A photograph showing the wing duct inlets and the manner in

which the airplane was mounted in the full-scale tunnel is presented in figure 3.

Instrumentation for Tests in the 40-by 80-Foot Wind Tunnel

A rake consisting of 29 total-head and 4 static-head tubes was placed in each oil-cooler duct at a station 18 inches behind the leading edge of the wing (sta. 1). An additional rake of 18 total-head tubes was mounted at the exit of each duct (sta. 2). These rakes furnished the data required to determine the pressure losses within the ducts, the quantity of flow, and the internal drag. A number of static-pressure orifices used to determine pressure distribution were installed at various points on the airplane, including points on the lips of the left-wing duct inlets.

Apparatus for 1/2-Scale-Model Investigation of Revised Inlets

The 1/2-scale models were supported and tested as illustrated in figure 4. Air flow through the 2- by 5-foot test section shown in this figure was obtained with a temporary setup which incorporated a blower normally utilized for ground tests of internal flow in duct systems. The tests were thus made with three-dimensional inlet models in an essentially two-dimensional flow. Satisfactory agreement with full-scale tests was obtained as shown later. Flow through the inlet of the duct models was induced by a jet pump capable of supplying a quantity of air flow variable from zero up to values corresponding to an inlet-velocity ratio of 0.92. At the center section of each model, numerous pressure orifices were installed around the airfoil contour and inside the duct lips. A rake of 26 total-head and 13 static-head tubes was placed at the same respective location as in the full-scale tests (sta. 1). Pressure measurements thereby furnished data for section lift coefficient, pressure recovery at station 1, and pressure distribution over the duct lips.

Ground-Test Apparatus

A 10-horsepower blower was used to induce flow through the ducts of the oil-cooler system. These tests were made using a production duct system with normal manufacturing roughness and incorporating a 21-1/2-inch by 10-3/8-inch by 9-inch elliptical oil cooler. In addition to rakes at stations 1 and 2, a set was installed at the face of the oil cooler. The test setup is shown in figure 5.

TESTS, RESULTS, AND DISCUSSION

The measurements in the 40- by 80-foot wind tunnel were first made with propellers removed in order to determine the air-flow characteristics in the absence of a slipstream. Following these measurements, data were taken with propellers operating in order to determine the effects of power as well as the air-flow characteristics that actually exist in flight. Instrumentation difficulties prevented the measurement of pressures at the face of the oil cooler; consequently the full-scale-airplane tests were limited to the determination of any losses due to the improper inlet design. It was left to the ground tests, therefore, to determine the losses in the turn from station 1 to the face of the oil cooler. The series of model tests were conducted on various revised inlets, because the full-scale-airplane tests disclosed excessive pressure losses occurring as a result of unsatisfactory inlet design.

Full-Scale Tests With Propellers Removed

This investigation was made in order to serve as a base for subsequent tests, as well as to determine the internal—flow and—drag characteristics of the oil—cooler ducts. The airplane was in the standard production condition with the exception that both propellers and spinners were removed (fig. 3). Pressure and force—test data were obtained throughout the angle—of—attack range at stream velocities of 80 and 125 miles per hour, and for various exit areas of the oil—cooler duct.

Figure 6 is a plot of the velocity distribution at station 1 in the left-wing duct for the entire angle-of-attack range and for an exit area of 80 square inches. The pressure recovery at

$$\frac{H - p_0}{q_0} = (1 - \Delta H/q_0) + \eta_0$$

Thus, for frictionless flow (no total-head loss) the coefficient $1-\Delta H/q_0$ is unity regardless of free-stream Mach number, whereas under the same conditions $(H-p_0)/q_0$ depends upon Mach number. Another form of pressure-recovery coefficient that is used in some reports is $(H-p_0)/q_{C_0}$, where $q_{C_0}=q_0(1+\eta_0)$. This coefficient, equal to $1-\Delta H/q_0$ differs from $1-\Delta H/q_0$ only in that the losses are expressed as a fraction of $q_0(1+\eta_0)$ instead of a fraction of q_0 .

In this report the pressure recovery at a station inside the duct is given by the coefficient $1-\Delta H/q_0$. For low free-stream Mach numbers this coefficient is the same as the more familiar coefficient $(H-p_0)/q_0$. The two are related by the equation

station l for various exit areas and various angles of attack is shown in figure 7. Velocity distributions and pressure recovery for the right-wing duct are not shown, since they are almost identical to those for the left wing. In figure 8 the flow parameter Q/V_0 is plotted as a function of the exit area A2 for angles of attack of 0° , 3° , and 8° . These angles correspond approximately to those for high speed, cruise, and climb. The internal drag of the left-wing duct for these same angles has been calculated using the relation

$$C_{D_i} = \frac{2Q}{SV_o} \left(1 - \sqrt{1 - \frac{\Delta H_2}{q_o}} \right)$$

and is presented in figure 9 as a function of exit area.

Several significant results can be obtained from the data of figures 6, 7, and 9. A separation of internal flow for angles of attack greater than 30 is indicated by the nonuniform velocity distribution of figure 6. These distributions clearly show that, in the absence of a slipstruam, separation occurs locally at the center of the lower intake lip for angles above 3° and progresses in width and height as a, is further increased. The loss in total head accompanying separation is verified by the low pressurerecovery coefficients of figure 7. It is seen from figure 9 that the internal-drag coefficient of both oil-cooler ducts is 0.0002 in high speed (approximated by $\alpha_{11} = 0^{\circ}$, $A_2 = 40$ sq in.) and 0.0023 in climb (approximated by $\alpha_{11} = 8^{\circ}$, $A_2 = 90 \text{ sq in.}$). These values compare with the total-drag measurements of the ducts, as determined by force tests, of 0 0002 in high speed and 0.0024 in climb. The increment of external drag due to the wing oil-cooler ducts is thus seen to be virtually zero.

Full-Scale Investigation With Power On

A series of tests similar to those made with propellers off was conducted with propellers operating, in order to determine the effect of power and internal—flow conditions that would exist in flight. In the wind tunnel, full—scale conditions for steady flight with normal rated power were reproduced up to a velocity of about 200 miles per hour. For flight conditions above this speed, the power coefficient, the thrust coefficient, and the V/nD ratio were still matched with the corresponding values in flight, but the tunnel velocity was held at 200 miles per hour. Figure 10 shows both the thrust coefficient and the uncorrected angle of attack as a function of lift coefficient for normal rated power.

Due to the difficulty of cooling the oil while operating in the tunnel, almost all data were taken with exit flaps full open. The results are presented as such, unless specifically noted to the contrary.

The velocity distributions at station 1 in the left-wing and right-wing ducts are shown in figures 11 and 12, respectively. As may be noted from figure 12, the distribution within the right-wing duct with power on is practically the same as the distribution in both ducts with propellers removed (fig. 6). However, a remarkable improvement resulted in the distribution within the left-wing duct (fig. 11). Additional corroboration of this dissimilar effect is given in figure 13, which shows average values of pressure recovery $1 - \Delta H/q_{\rm O}$ and of flow parameter $Q/V_{\rm O}$ plotted as a function of $\alpha_{\rm U}$ for normal rated power. For purposes of comparison, the corresponding power-off data for both ducts are also included.

From these figures it is seen that with power on separation occurs over the lower lip of the right-wing inlet for angles greater than $\alpha_u=4^\circ$. This is the same as the power-off data. In the left-wing inlet, however, there is no separation of internal flow even for angles as high as $\alpha_u=10^\circ$. These dissimilar effects are a consequence of the opposite slipstream rotation for the two inlets. A more detailed consideration of their significance is given in a subsequent section of the discussion.

Because separation of internal flow is indicated on a manometer board by the sudden changes in fluid height, the cooling difficulties associated with it are readily detected by full-scale operation in the wind tunnel. In this way the correlation of separation with excessive oil temperatures and the dissimilarity of the slipstream effects were noticed many times during the power-on tests. As α_u was increased, the right-engine oil temperature became excessive, but the left did not. When such a condition existed, the flow in the right duct was always separated, but the flow in the left duct was not (as indicated by the various fluid heights). In order to decrease the oil temperature to a value below the limit, the power was reduced. Whenever the power was suddenly reduced, it was always noticed that simultaneously the air flow in the left duct separated, thus giving a visual indication of the beneficial effect of power on the flow conditions in the left duct.

Tests of 1/2-Scale Models of Various Modified Inlets

From figure 13 it can be seen that proper modifications to the right duct would increase the pressure recovery at the cooler approximately 0.6 q_0 at $C_L=0.94$. An investigation of various models was made, therefore, to determine the duct—lip modifications which would be necessary in order to eliminate the stall of the lower lip of the right—hand duct. As previously described, the revised inlets were tested on models in a two—dimensional—flow test section. The tests were made throughout the angle—of—attack range at a q_0 of approximately 28 pounds per square foot, which corresponds to a Reynolds number of 5,500,000, based upon the 66.7—inch chord of the models.

For each model tested, the inlet-velocity ratio was varied with c_l in order to simulate a constant quantity of flow of approximately 400 pounds per minute at sea level. The section lift coefficient c_l at a station through the center of the duct was used as the fundamental parameter to describe the inlet attitude. It is to be distinguished from the airplane lift coefficient C_L . The relationship between c_l and C_L , shown in figure 14, was determined from earlier pressure distribution measurements and force tests of the airplane. The variation of $V_{\dot{l}}/V_{0}$ with c_l necessary to simulate a flow of 400 pounds per minute is also shown in figure 14^{1} .

For convenience, the upper—and lower—duct lips are designated by the letters U and L, respectively. The various modifications of these lips are designated by a digit following the letter. Thus, UOL3 represents a model consisting of the original upper lip and the third revised lower lip. The profiles of the various modifications are given in figure 15, which is a scale drawing of a section through the center of the wing inlet. Ordinates for these profiles are given in table I.

For purposes of comparison, the pressure recoveries at station 1 for the various ducts are shown on the same plot (fig. 16) as a function of c_l . As may be noted from this figure, a marked improvement in pressure recovery at high c_l 's was obtained with the modified ducts. Further confirmation of these improvements is given in figure 17, which compares the velocity distributions of UOL1 (essentially the original duct) with those of the optimum duct UIL5.

It was intended that UOL1, the first inlet tested, be a 1/2-scale model of the original inlet UOL0, but due to an error in model layout the lower lip L1 was constructed as shown in figure 15. Because L1 was cut back a little more than L0 and possessed slightly more positive camber, the duct UOL1 showed slightly better pressure recovery at high values of c_1 than did UOL0 (fig. 16). Considering this discrepancy in model construction, there is good agreement

Other tests have shown that the pressure recovery, particularly at high lift coefficients, can often be seriously affected by the inlet-velocity ratio. The effects of this variable were investigated at several lift coefficients for the original and modified inlet designs. The effect was found to be negligible in the case of the revised inlets, and therefore the major portion of the data was obtained for the $\rm V_i/\rm V_0$ ratio shown in figure 14. The results showed, for example, that an increase in inlet velocity from 0.6 to 0.9 altered the pressure recovery less than 2 percent at lift coefficients near 1.0. The original was more critical in this regard showing a 7-percent decrease in pressure recovery under these same conditions.

between the full-scale airplane tests and the tests of models in two-dimensional flow.

From figure 16 it is seen that several of the ducts (e.g., UOL4, U1L4, U1L5) yield almost equally satisfactory pressure recovery over the c_l range from high speed ($c_l \cong 0.17$) to climb ($c_l \cong 0.85$). The duct U1L5, however, is considered as the optimum of the modifications tested because it has a somewhat higher critical speed than do the others. The inlet U1L4 is considered as an alternate, because it requires less change in the original lip contours than does U1L5. Using the Kármán-Tsien method, the peak pressures correspond to a critical Mach number of 0.56 for the original duct, 0.56 for the alternate duct, and 0.59 for the optimum duct. In each case the peak-pressure region is confined to a very small area on the outside of the lower lip, and is not considered to be of importance.

Ground Tests of Duct Passages

Since the majority of duct expansion occurred in the turn ahead of the oil cooler, it was considered a possible source of excessive pressure losses. Consequently, the ground tests were conducted on the production duct from station 1 to the exit of the oil cooler. The blower used to induce flow through the system provided an air flow of 200 pounds per minute, which is approximately one—half the actual flow that exists in climbing flight.

An investigation was first conducted on the duct passages as fabricated for production airplanes. These tests indicated that, with a uniform velocity distribution ahead of the turn, the average pressure loss from station 1 to the face of the oil cooler is 0.089q1. Measurements of the production—duct system showed that its contours deviated considerably from the production drawings. These deviations were as follows: (1) the inside turn of the inner compartment was sharper, (2) the inner wall of the inner turn projected 5/16 inch nearer to the center of the duct, and (3) the forward end of the inside vane was 1/2 inch closer to the inside wall.

The average pressure loss in the turn was reduced to 0.054q₁ by modifying the inside radius of the inner compartment and by changing the location of the inner vane. These modifications, which produced minimum losses, resulted in a final turn with contours conforming almost exactly to the blueprints.

Thus, the losses in the turn are quite small, even with considerable production irregularities in the fabricated parts. The difficulty in oil cooling, therefore, is not a consequence of excessive pressure losses in the diffuser ahead of the oil cooler.

The Effects of Power

The model tests have shown that in the absence of a slipstream either of the revised inlets UlL4 or UlL5 could be used in the right-wing duct to produce practically complete pressure recovery and uniform velocity distribution at station 1. The full-scale airplane tests have shown that the existing design of the left-wing inlet is adequate with power on (although it would appear to be unsatisfactory from power-off tests) because of the large beneficial effect of the slipstream. Consequently, an explanation is required to justify the direct application of the model tests (which were conducted in the absence of the slipstream) to the conditions of the right-wing inlet with propellers operating.

The critical attitude for flow conditions in the right inlet is at a high angle of attack. Here the slipstream effects are large, and separation of internal flow over the lower lip is critical. In figure 18 a diagram is presented which illustrates how rotation of the propellers produces a very different effect on the air as it approaches the two opposite sides of a nacelle. The analysis is admittedly simplified, but nevertheless illustrates how the resultant velocity of the air entering the inlets, when compared to power-off condition, is at a considerably lower angle of attack on the side of downgoing blades, and yet is practically at the same angle of attack on the side of the upgoing blades. These statements are verified by the full-scale airplane tests of this report. That is, the angle of impending separation in the right-wing inlet (on side of the upgoing blades) was the same with propellers off as with propellers operating (fig. 13), yet the separation in the left-wing inlet (on side of downgoing blades), which began at $\alpha_1 = 3^{\circ}$ with the propellers removed, did not occur at all with propellers operating. The separation criterions obtained in the 1/2-scale model tests, therefore, are directly applicable to the power-on conditions of the right-wing inlet.

It is realized that in modifying an inlet for the purpose of extending the range of good pressure recovery to higher c_l's, it is easily possible to go too far in the design so that separation of internal flow would occur over the upper lip at low angles of attack (e.g., trend of recovery characteristics shown by duct UOL4 in fig. 16). However, low angles of attack correspond to high speeds, where the slipstream effects are very small. Consequently, power—off data can also be applied to the high-speed condition with only small corrections necessary for the slight increase in ram caused by the propellers.

In general, then, it can be expected that inlets which are similar to the ones on the test airplane, and which produce satisfactory pressure recovery throughout the operating range when tested with propellers removed, will do likewise when tested with propellers operating, irrespective of whether they are behind

upgoing or downgoing blades. The converse of this statement cannot be applied to inlets behind downgoing propeller blades. That is, such an inlet, which does not yield adequate pressure recovery at high angles when tested without propellers, may yield complete pressure recovery when the propellers are operating. Figures 6 and 11 are remarkable evidence of this statement.

CONCLUDING REMARKS

- 1. In the high-speed attitude, no increase in external drag was caused by the wing-inlet ducts. In the climb attitude, an increment of 0.000l can be attributed to external drag of these ducts.
- 2. The excessive pressure losses in the right-wing inlet were due to improper inlet design, and not due to high losses in the duct passages. The losses in the expanding turn ahead of the oil cooler were small.
- 3. The modified right-wing inlet, developed by model tests, produced a ducting system with good pressure recovery and uniform velocity distribution throughout the range from high speed to climb.
- 4. Wing inlets which are to be placed behind upgoing propeller blades will produce approximately the same degree of pressure recovery at high angles of attack in flight that they produced when tested with propellers removed. However, the pressure recovery of an inlet which is to be placed behind the downgoing blades will be considerably better when tested at high angles of attack with power on than when tested at the same angle of attack with propellers removed.
- 5. The correlation between the results of this investigation and the reported data from flight tests is good. Available flight-test data show that in climb to high altitudes the left-engine oil temperature (on side of downgoing blades) ordinarily stays within the safe limit, but the right-engine oil temperature (on side of upgoing blades) becomes excessive.
- 6. Because the charge-air wing inlets on the test airplane are similar to the oil-cooler inlets, and because they are outboard of the nacelles instead of inboard, it is expected that modifications to the left-wing charge-air inlet similar to those recommended herein for the right-wing oil-cooler inlet will effect a comparative increase in ram at high angles of attack.

Ames Aeronautical Laboratory,
National Advisory Committee for Aeronautics,
Moffett Field, Calif., March 10, 1945.

REFERENCE

1. Allen, H. Julian, and Vincenti, Walter G.: Wall Interference in a Two-Dimensional-Flow Wind Tunnel With Consideration of the Effect of Compressibility. NACA ARR No. 4KO3, 1944.

TABLE I.— ORDINATES OF VARIOUS LIPS AT CENTER OF WING INLET [Stations are given in in. behind the O-percent-chord line. Ordinates are given in in., measured perpendicular to chord line. Chord = 66.7 in.]

17		Lip Ll		Tim IS		7.						
	LIP LL			Lip L5			Lip Ul			Lip UO		
	Station	Upper	Lower	Station	Upper	Lower	Station	Upper	Lower	Station	Upper	Lower
	0.79 .80 .85 .90 1.00 1.20 1.40 1.70 2.00 2.50 3.00 4.00 5.00 6.00 7.00	1.38 1.31 1.25 1.21 1.17 1.12 1.08 1.03 .99 .92 .88 .86 .88	1.38 1.44 1.53 1.59 1.68 1.80 1.90 2.00 2.08 2.19 2.30 2.48 2.64 2.78 2.90	2.39 2.45 2.50 2.60 2.70 2.80 2.90 3.00 3.20 3.50 4.00 4.50 5.00 6.00 7.00	1.68 1.54 1.48 1.40 1.33 1.27 1.22 1.17 1.07 .98 .89 .88	1.68 1.80 1.85 1.91 1.96 2.00 2.03 2.07 2.13 2.21 2.34 2.45 2.56 2.75 2.90	-0.1005 .00 .10 .30 .60 1.50 2.00 3.00 4.00 5.00 6.00 7.00	2.07 2.29 2.38 2.50 2.73 2.98 3.24 3.50 3.76 4.13 4.47 4.77 5.03 5.25	2.07 1.86 1.81 1.73 1.65 1.58 1.55 1.55 1.59 1.72 1.91 2.11 2.33 2.53	-0.1005 .00 .10 .30 .60 1.50 2.00 3.00 4.00 5.00 6.00 7.00	2.07 2.29 2.38 2.50 2.73 2.98 3.24 3.50 3.76 4.13 4.47 5.03 5.25	2.07 1.86 1.81 1.75 1.71 1.68 1.69 1.73 1.80 1.93 2.08 2.24 2.40 2.56
+		Lip		Lip L3				Lip L4				
	Station	Up	per	Lower	Station	U	pper	Lower	Stat	ion I	Jpper	Lower
THE MO. POOLO	1.83 1.86 1.90 2.00 2.20 2.50 3.00 4.00 5.00	1. 1. 1	1.52 1.36 1.29 1.18 1.07 .98 .91 .86		1.93 1.96 2.00 2.10 2.20 2.50 3.00 4.00 5.00	1 1 1 1 1 1 1	.78 .65 .59 .46 .39 .24 .07 .88	1.78 1.90 1.95 2.03 2.09 2.19 2.30 2.48 2.64	2.3 2.4 2.4 2.5 2.6 2.7 3.0 3.5 4.0	0 3 5 6 6 6 6 6 6 6 6 6	1.90 1.79 1.71 1.66 1.57 1.51 1.33 1.11 1.98	1.90 2.01 2.08 2.10 2.15 2.19 2.28 2.39 2.48 2.64

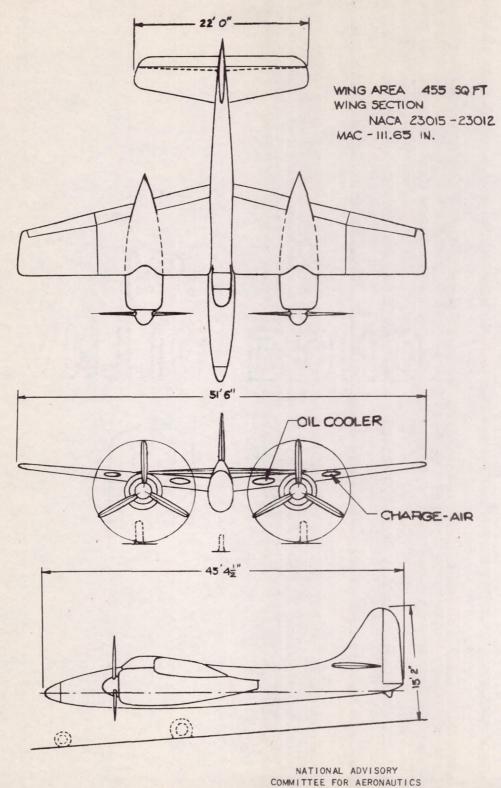
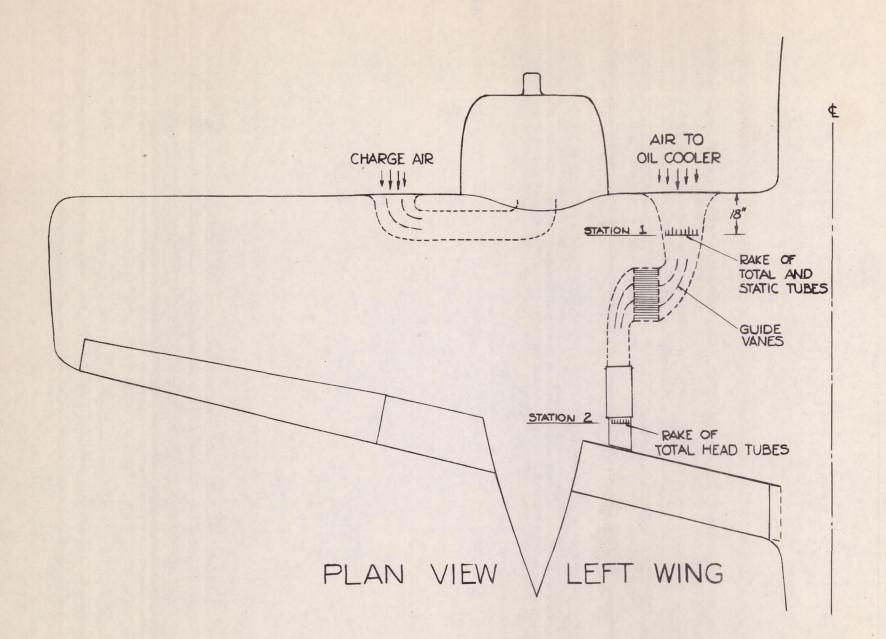


FIGURE 1 .- THREE VIEWS OF THE TEST AIRPLANE



NATIONAL ADVISORY COMMITTEE FOR AERONAUTICS

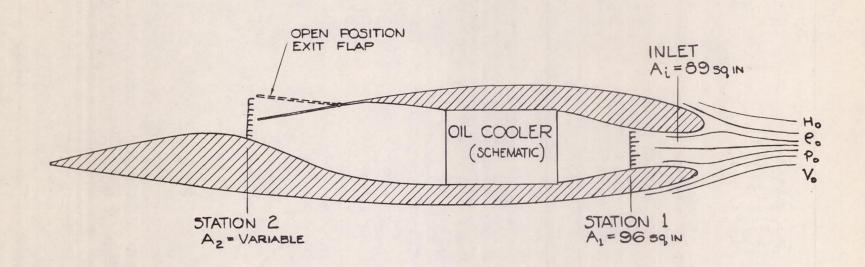


FIGURE 2 - INSTALLATION OF PRESSURE-TUBE RAKES IN OIL-COOLER DUCT

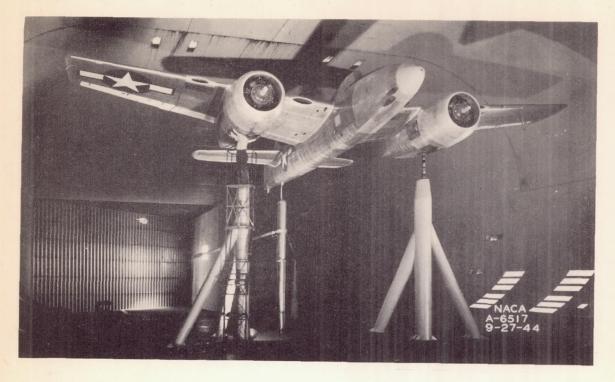
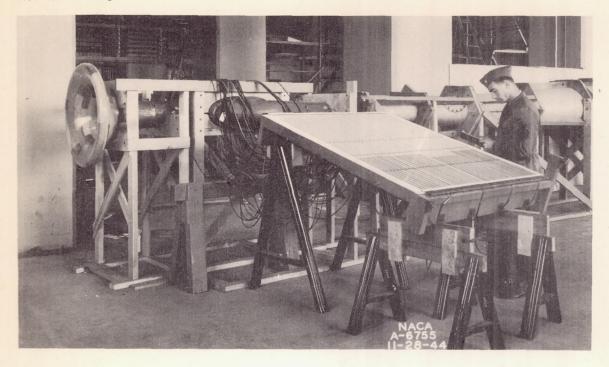


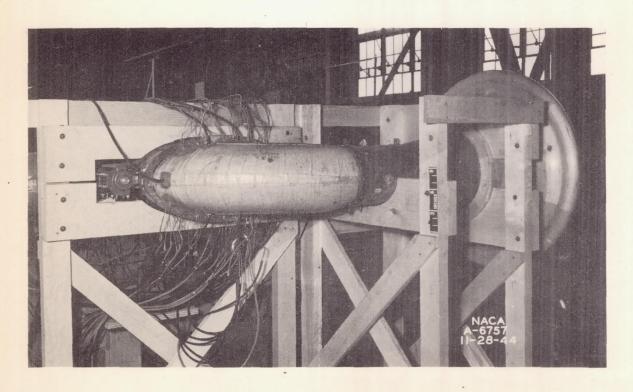
Figure 3.- The test airplane mounted in the Ames 40- by 80-foot wind tunnel.



Figure 4.- Installation of the model of the wing-inlet used in two-dimensional-flow tests.



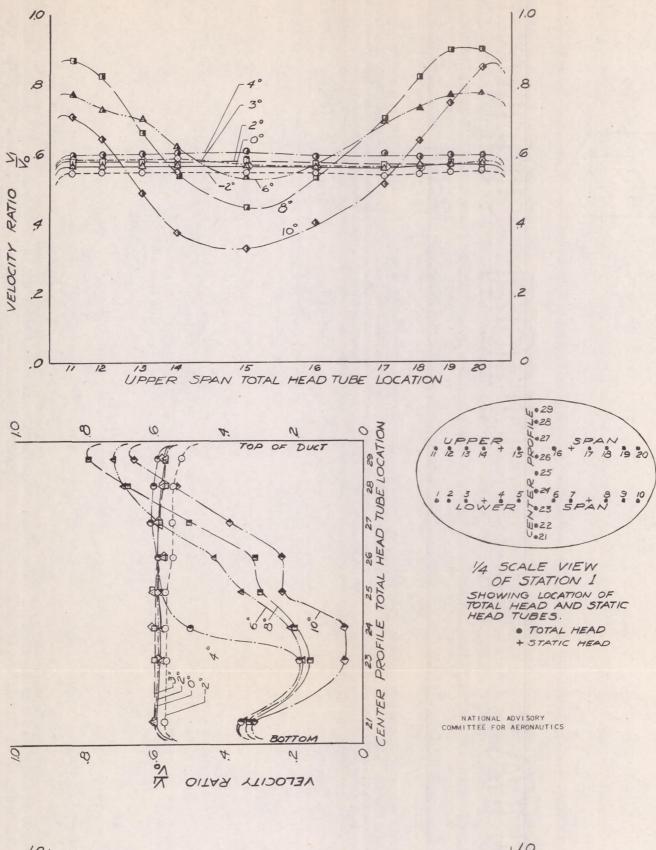
(a) General arrangement.



(b) Pressure-tube rake installations at face of oil cooler.

Figure 5.- Apparatus for ground tests of oil-cooler duct.





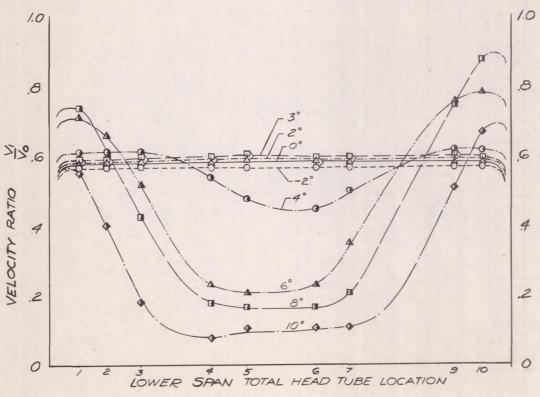
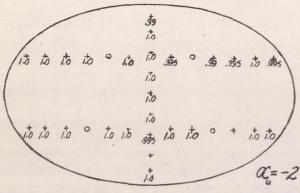
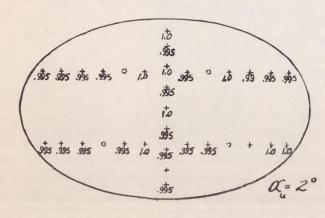
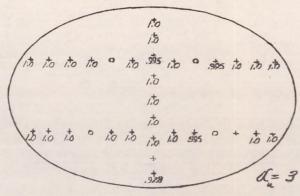


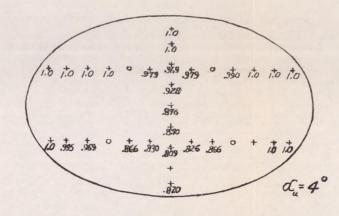
FIGURE 6. - VELOCITY DISTRIBUTION IN LEFT WING OIL-COOLER DUCT
POWER OFF, DUCT-EXIT AREA, 80 SQ IN.; 9, 40 LB/SQ FT

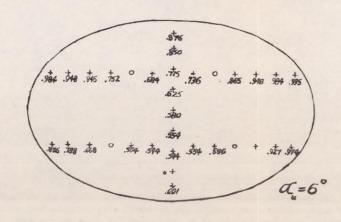




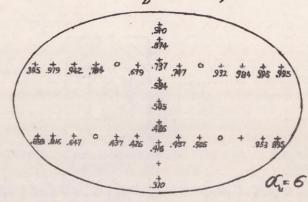
RUN 4 EXIT AREA 52.5 IN 2 9 = 40 16/ft 2

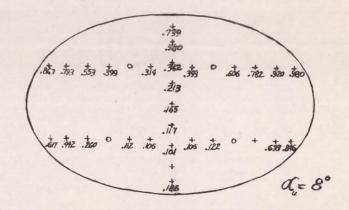


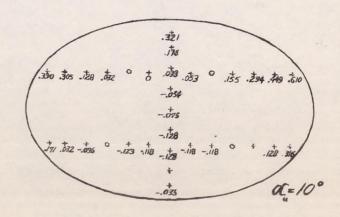




RUN 6 EXIT AREA 80 IN 2 9=40 16/ft2







NUMBERS REPRESENT PRESSURE RECOVERY COEFFICIENT (1- AH)

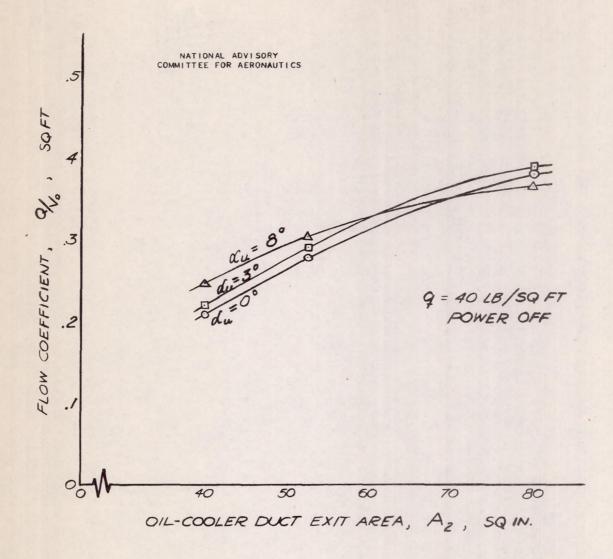


FIGURE 8.- QUANTITY OF AIR FLOW THROUGH LEFT WING OIL-COOLER
DUCT

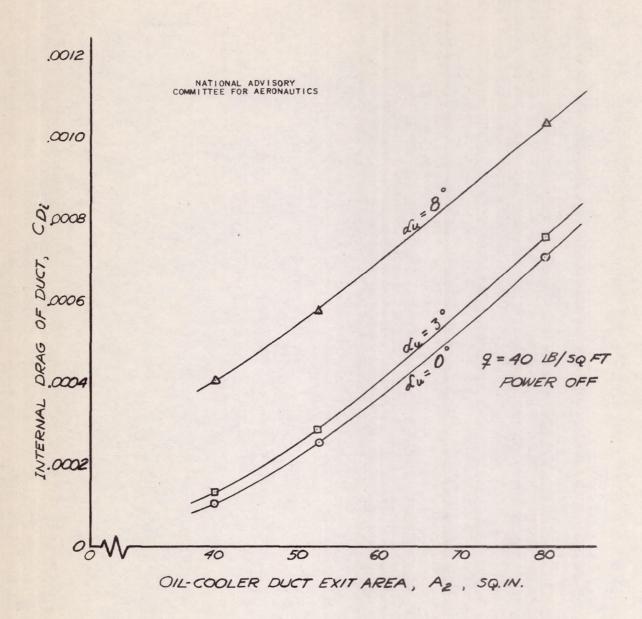


FIGURE 9 .- INTERNAL DRAG OF LEFT WING OIL-COOLER DUCT.

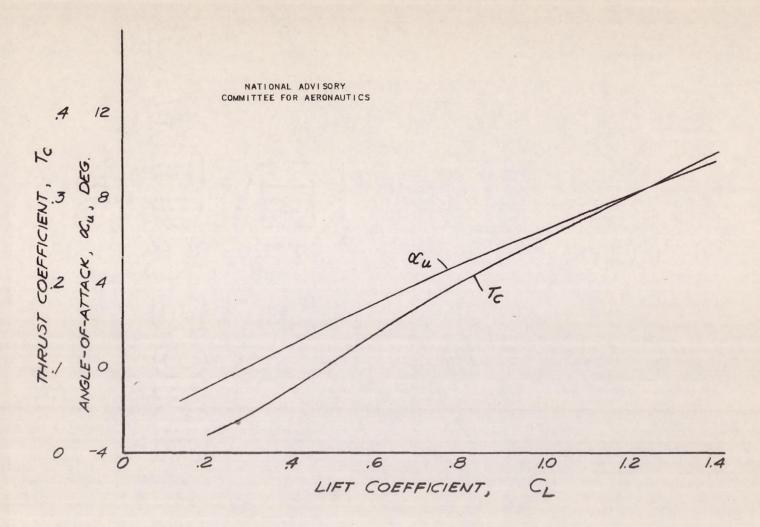
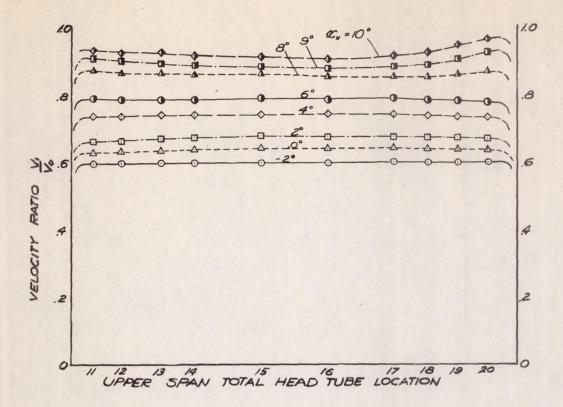
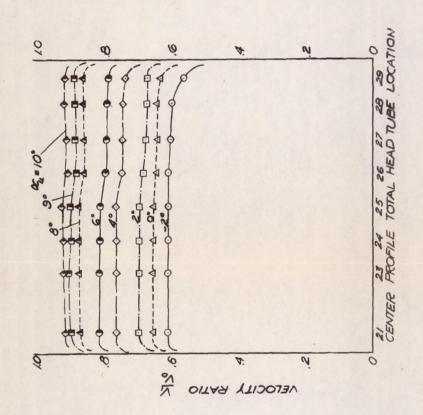
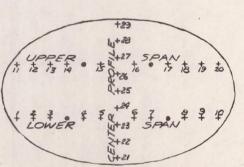


FIGURE 10.- THRUST COEFFICIENT AND ANGLE-OF-ATTACK AS A FUNCTION OF LIFT COEFFICIENT. NORMAL RATED POWER,







VIEW LOOKING DOWNSTREAM, STATION I PRESSURE TUBE LOCATION IN LEFT WING DUCT + TOTAL HEAD TUBE • STATIC TUBE

NATIONAL ADVISORY COMMITTEE FOR AERONAUTICS

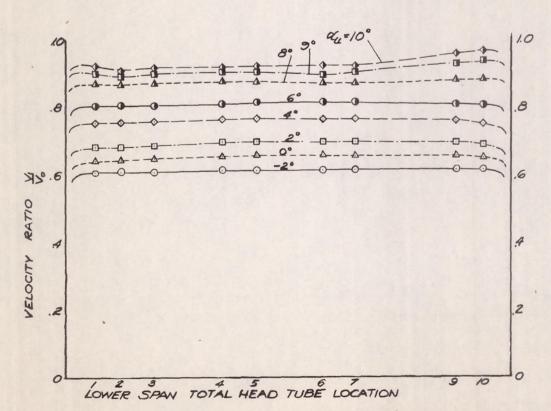


FIGURE 11.- VELOCITY DISTRIBUTION IN LEFT-WING OIL-COOLER DUCT NORMAL RATED POWER.

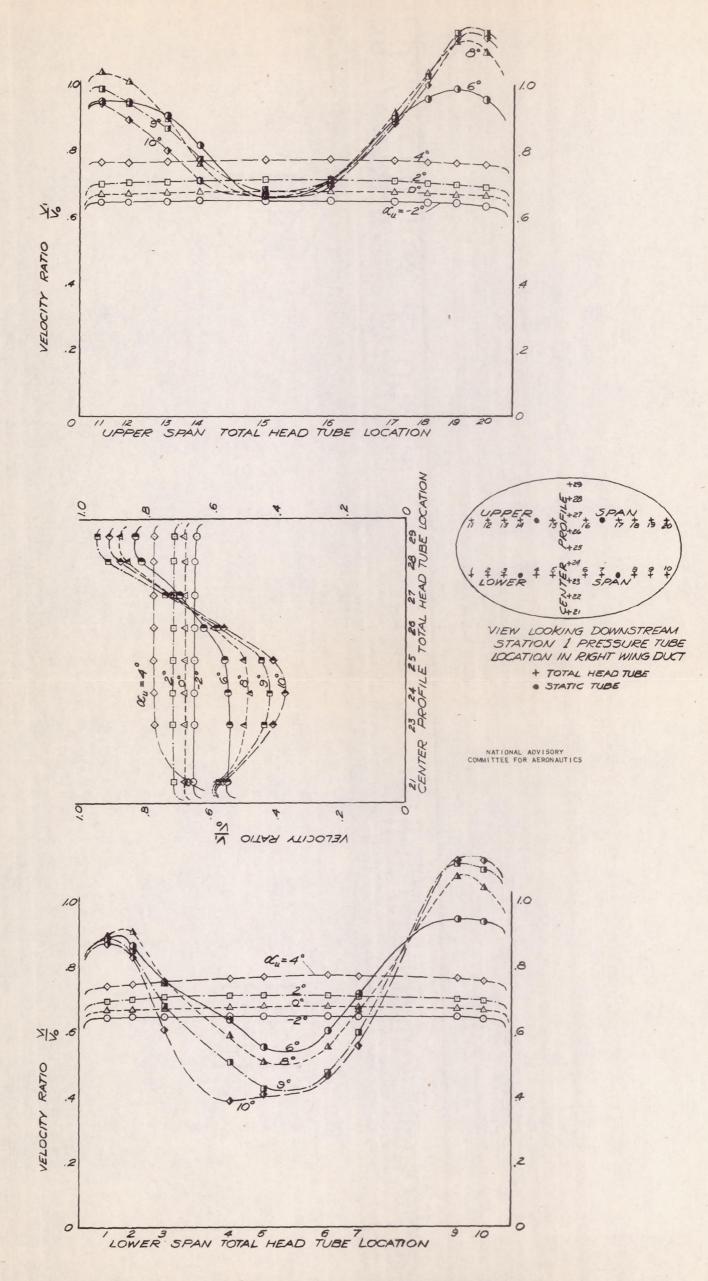
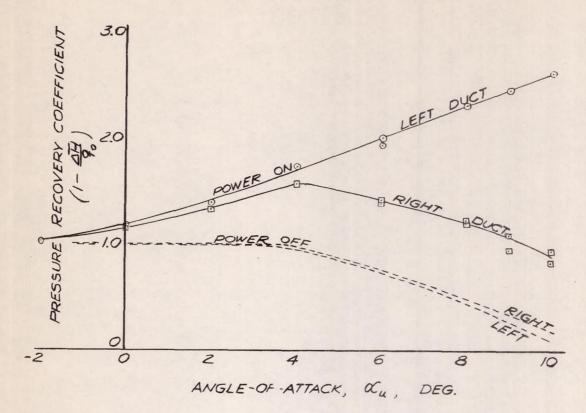


FIGURE 12 - VELOCITY DISTRIBUTION IN RIGHT WING OIL-COOLER DUCT.

NORMAL RATED POWER.



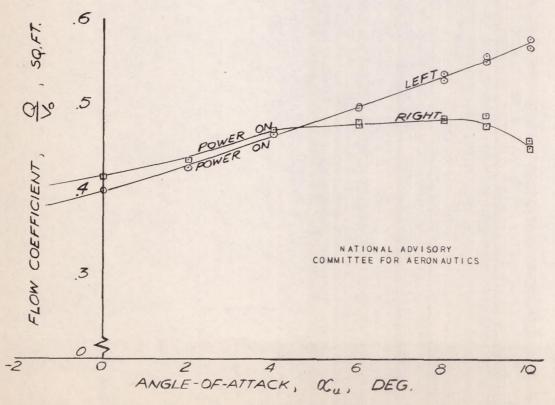
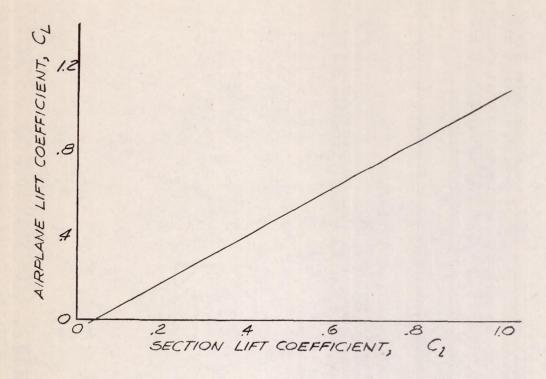


FIGURE 13.- PRESSURE RECOVERY AND QUANTITY OF FLOW.

NORMAL RATED POWER,



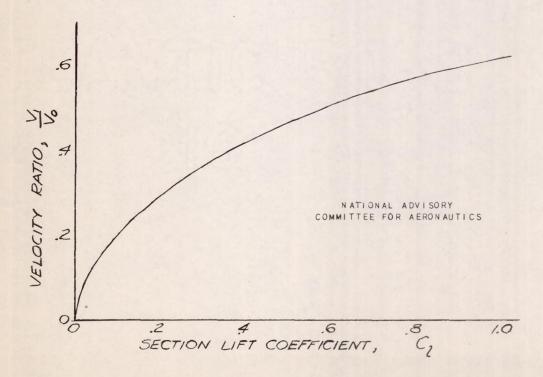


FIGURE 14. - VARIATION OF AIRPLANE LIFT COEFFICIENT AND VELOCITY RATIO WITH SECTION LIFT COEFFICIENT AT CENTER OF OIL-COOLER DUCT

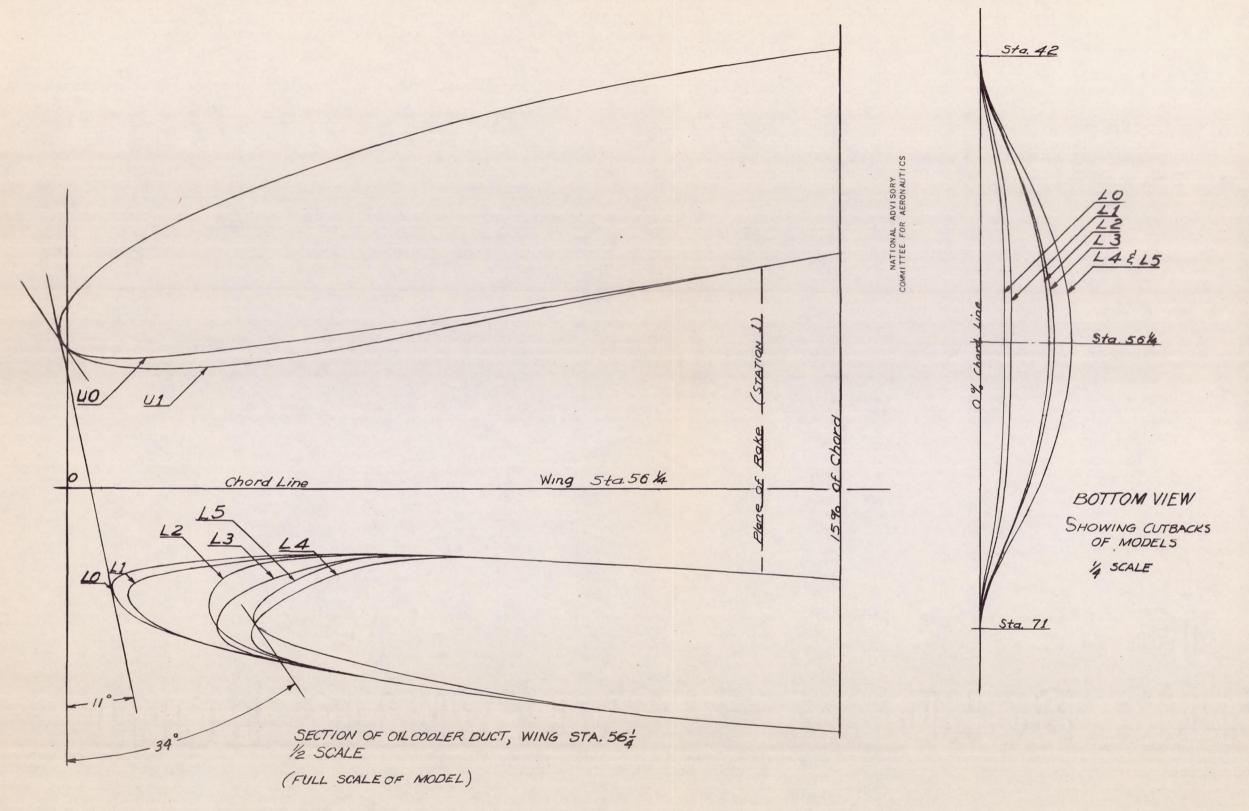


FIGURE 15.- SCALE DRAWING OF VARIOUS DUCT LIPS OIL-COOLER-DUCT MODELS.

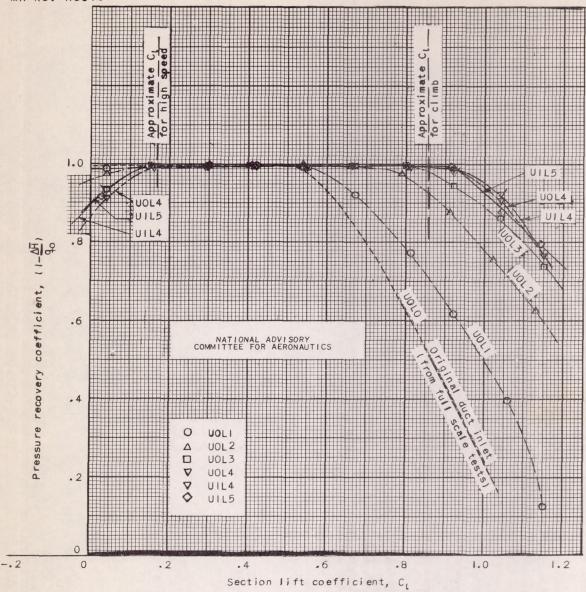
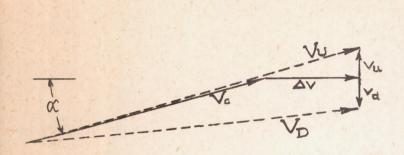
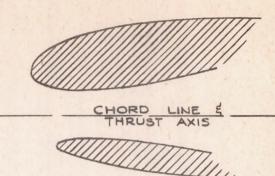


Figure 16. - Pressure recovery at station I vs section lift coefficient, for the various duct lips of the oil-cooler inlet.

FIGURE 17. - VELOCITY PROFILES IN ORIGINAL AND FINAL MODIFIED DUCTS.

BOTTOM WALL





- Vo free stream velocity, approaching inlet at angle €
- AV axial increment of velocity induced by propeller (assumed to be parallel to thrust axis)
 - vu rotational component of velocity induced by UP-GOING propeller blades
 - vd rotational component of velocity induced by DOWN-GOING propeller blades
 - Vu RESULTANT velocity entering the inlet which is behind UP-GOING blades
 - VD RESULTANT velocity entering the inlet which is behind DOWN-GOING blades

NATIONAL ADVISORY COMMITTEE FOR AERONAUTICS

FIGURE 18 - SKETCH ILLUSTRATING EFFECT OF SLIPSTREAM
ROTATION ON THE VELOCITY APPROACHING AN INLET.